Generalized Clock Models[1]

Leon Hostetler [1], Jin Zhang [2], Ryo Sakai [2],
Judah Unmuth-Yockey [3], Alexei Bazavov [1], and Yannick Meurice [2]

[1] Michigan State University

[2]University of Iowa

[3]Fermilab

July 13, 2021
QuLAT Collaboration

[1]arXiv:2105.10450

Outline

Motivation

- Ultimately, we want to do quantum simulation of lattice QCD
- First, we must be able to do this with simpler Abelian models
- Given the limited number of qubits available, it is important to optimize the discretization procedure
- One can make a $\mathbb{Z}_q$ approximation of a continuous $U(1)$ symmetry
- To optimize such a $\mathbb{Z}_q$ approximation, it is useful to build a continuous family of models that interpolate among the various possibilities
- This brings us to our extended-$O(2)$ model

The Extended-O(2) Model

- We consider an extended-O(2) model in 2D with action

$$S_{\text{ext-}O(2)} = -\beta \sum_{x,\mu} \cos(\varphi_{x+\hat{\mu}} - \varphi_x) - \gamma \sum_x \cos(q\varphi_x)$$

- When $\gamma = 0$, this is the classic XY model, with a BKT transition
- When $\gamma > 0$, the second term breaks periodicity and we must choose $\varphi \in [\varphi_0, \varphi_0 + 2\pi)$ for some choice φ_0
- When $\gamma \to \infty$, the continuous angle φ is forced into the discrete values

$$\varphi_0 \leq \varphi_{x,k} = \frac{2\pi k}{q} < \varphi_0 + 2\pi$$

  - For $q \in \mathbb{Z}$, this is the ordinary q-state clock model with $\mathbb{Z}_q$ symmetry
  - For $q \notin \mathbb{Z}$, this defines an interpolation of the clock model for noninteger q

Some Monte Carlo Results

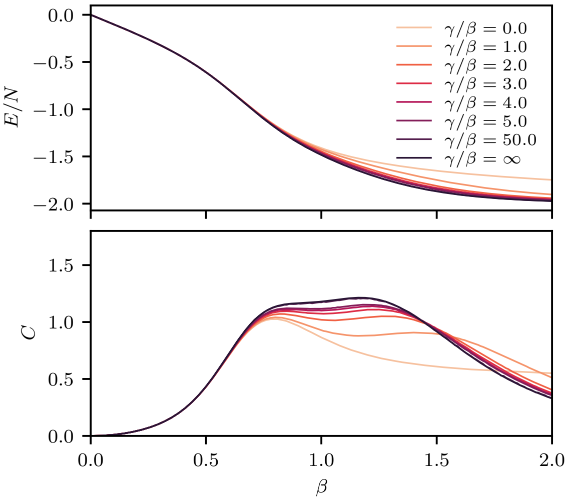

Figure: Results from a Metropolis algorithm on a 4×4 lattice with $q = 5.0$.

The Extended-q Clock Model

- In the limit $\gamma \to \infty$, we can replace the action with

$$S_{\text{ext-}q} = -\beta \sum_{x,\mu} \cos(\varphi_{x+\hat{\mu}} - \varphi_x)$$

- We directly restrict the previously continuous angles to the discrete values

$$\varphi_0 \leq \varphi_{x,k} = \frac{2\pi k}{q} < \varphi_0 + 2\pi$$

- We choose $\varphi_0 = 0$, i.e. $\varphi \in [0, 2\pi)$, but we also investigate $\varphi_0 = -\pi$
- For $q \notin \mathbb{Z}$, divergence from ordinary clock model behavior is driven by the introduction of a "small angle":

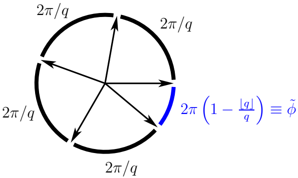

Monte Carlo results at small volume

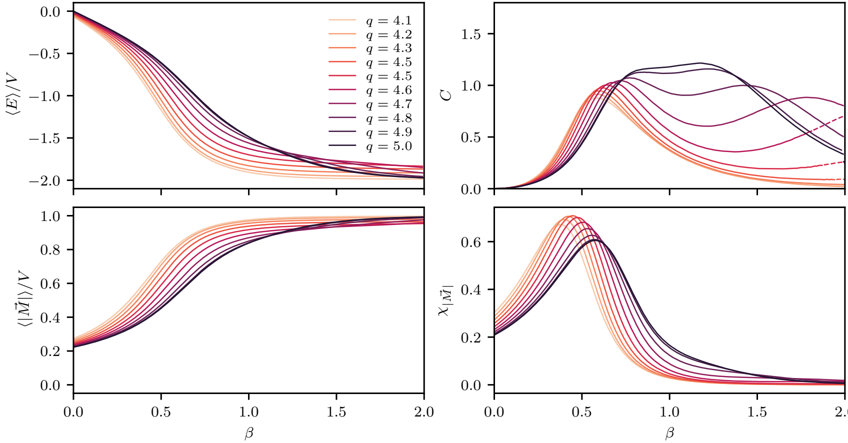

Figure: Results for the extended-q clock model from a heatbath algorithm on a 4×4 lattice.

Phase transitions for $q \in \mathbb{Z}$

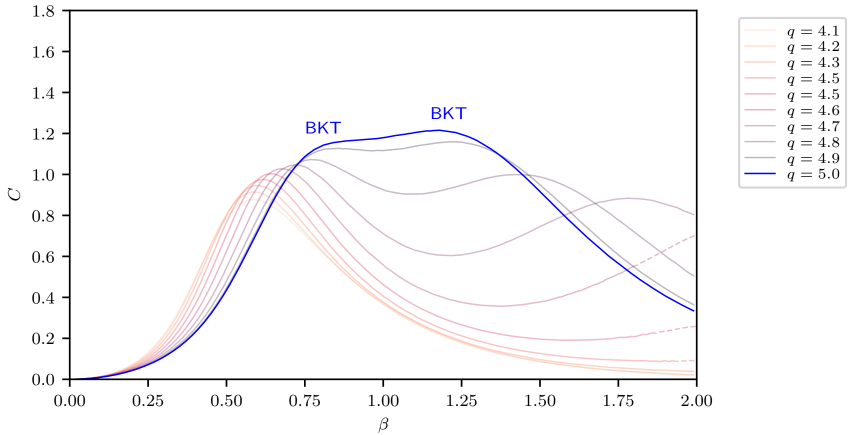

Figure: For integer $q \geq 5$, both peaks in the specific heat are associated with BKT transitions (see Li et. al. in Phys. Rev. E **101**, 060105(R) (2020)).

Phase transitions for $q \notin \mathbb{Z}$ (?)

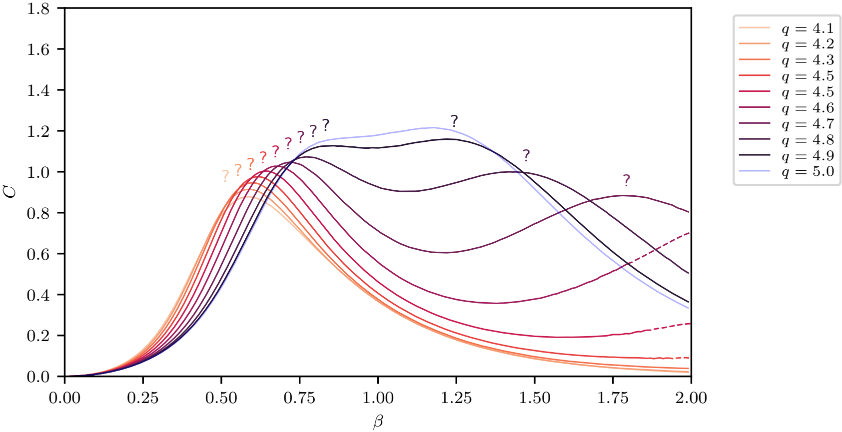

Figure: For non-integer q, are these also BKT transitions or are they something else?

TRG

- In the Monte Carlo approach, we use a Markov chain importance-sampling algorithm to generate equilibrium configurations
  - Unfortunately, in this model for non-integer q and large β, the configuration space splits into two sectors and the Markov chain tends to get stuck in one or the other
  - Monte Carlo has difficulty sampling this model appropriately at $\beta > 1$ for $q \notin \mathbb{Z}$
  - Integrated autocorrelation time explodes, and we have to perform billions of heatbath sweeps already on a 4×4 lattice
  - Studying this model on larger lattices with Monte Carlo is challenging
- Tensor renormalization group (TRG) approach can be used instead
  - We validate TRG against Monte Carlo in the regime accessible to Monte Carlo
  - Then we use TRG to explore lattice sizes and β-values beyond the reach of Monte Carlo

TRG results at large volume

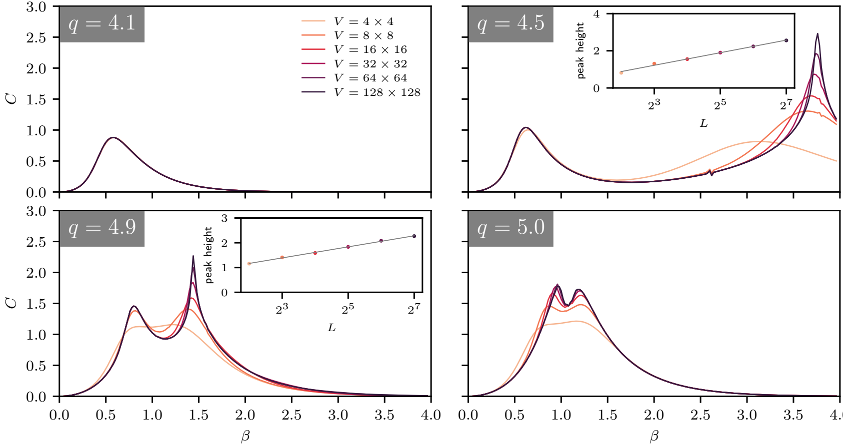

Figure: Specific heat results for the extended-q clock model from TRG obtained by Ryo for $q = 4.1$, 4.5, 4.9, and 5.0 at volumes from $2^2 \times 2^2$ up to $2^7 \times 2^7$.

Phase transitions for $q \notin \mathbb{Z}$

- First peak in specific heat:
  - Magnetic susceptibility converges to a finite constant as $H \to 0$
  - Magnetic susceptibility converges to a finite constant as $V \to \infty$
  - $\implies$ Not a phase transition
- Second peak in specific heat:
  - Looking at the magnetization vs. magnetic susceptibility gives result consistent with $\delta = 15$
  - Finite size scaling of magnetic susceptibility gives result consistent with $\gamma = 7/4$
  - $\implies$ Ising phase transition

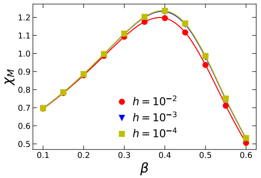

Example from TRG with $q = 4.3$ showing χ_M going to a constant as external field is taken to zero.

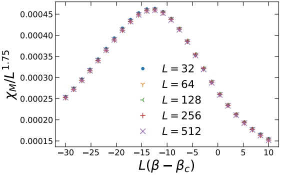

Example from TRG with $q = 4.3$ showing that volume dependence of χ_M is consistent with $\gamma = 7/4 = 1.75$.

Phase diagram for $\gamma = \infty$ and $\varphi_0 = 0$

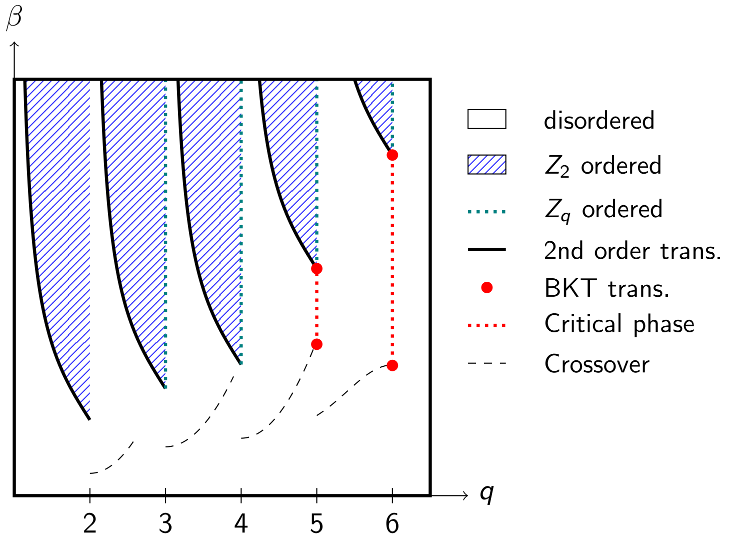

Summary & Outlook

1. We looked at an extended O(2) model with parameters β, γ, and q

$$S = -\beta \sum_{x,\mu} \cos\left(\varphi_{x+\hat{\mu}} - \varphi_x\right) - \gamma \sum_x \cos(q\varphi_x)$$

2. We learned enough to establish the $\gamma = \infty$ slice of the 3D phase diagram
   - When $q \in \mathbb{Z}$, we recover the classic q-state clock model which has a single second-order phase transition for $q = 2, 3, 4$ and two BKT transitions for $q \geq 5$
   - When $q \notin \mathbb{Z}$, we get a crossover and a second-order phase transition
3. We want to look at finite γ

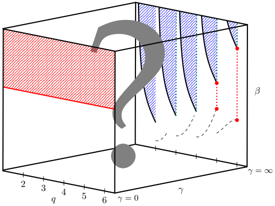

Summary & Outlook

4. This model may be a good candidate for analog quantum simulation as a small step toward the ultimate goal of simulating QCD on a quantum computer
5. Perhaps on Rydberg arrays. See (Keesling et. al. Nature **568**, 207 (2019))

Thank you!

Additional Slides:

Overview

Some Monte Carlo Results

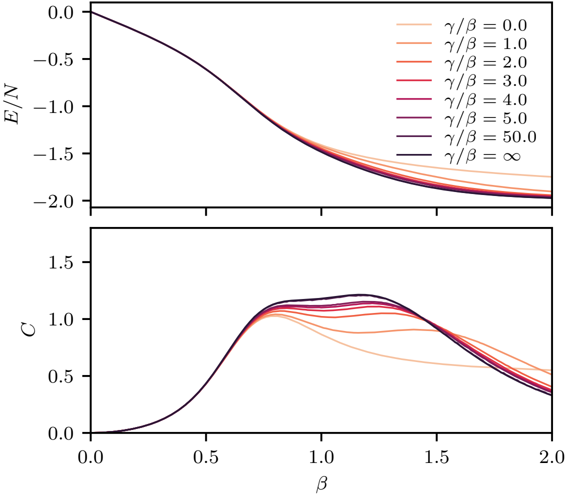

Figure: Results from a Metropolis algorithm on a 4×4 lattice with $q = 5.0$.

Some Monte Carlo Results

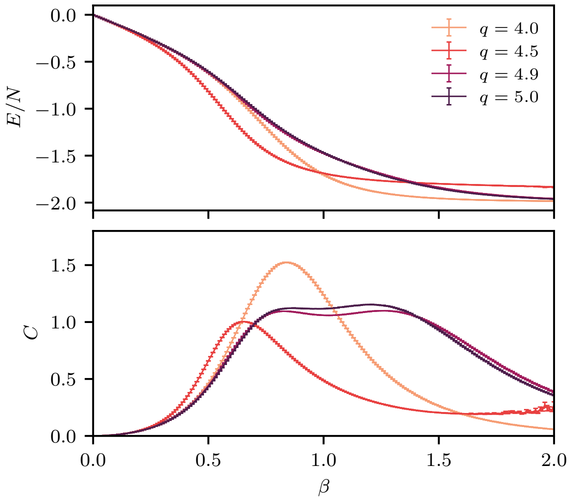

Figure: Results from a Metropolis algorithm on a 4×4 lattice with $\gamma/\beta = 5.0$.

Overview

Definitions

Internal energy

$$\langle E \rangle = -\frac{\partial}{\partial \beta} \ln Z = -\langle S \rangle$$

Specific heat

$$C = \frac{1}{V} \frac{\partial \langle E \rangle}{\partial T} = \frac{\beta^2}{V} (\langle S^2 \rangle - \langle S \rangle^2)$$

Magnetization

$$\langle \vec{M} \rangle = \frac{1}{\beta} \frac{\partial}{\partial \vec{H}} \ln Z = \left\langle \sum_x \vec{s}_x \right\rangle$$

Magnetic susceptibility

$$\chi_{\vec{M}} = \frac{1}{V} \frac{\partial \langle \vec{M} \rangle}{\partial \vec{H}} = \frac{\beta}{V} \left(\langle |\vec{M}|^2 \rangle - \left| \langle \vec{M} \rangle \right|^2 \right).$$

Proxy magnetization and susceptibility

$$\langle |\vec{M}| \rangle = \left\langle \left| \sum_x \vec{s}_x \right| \right\rangle, \qquad \chi_{|\vec{M}|} = \frac{\beta}{V} \left(\langle |\vec{M}|^2 \rangle - \langle |\vec{M}| \rangle^2 \right)$$

Energy Density from TRG

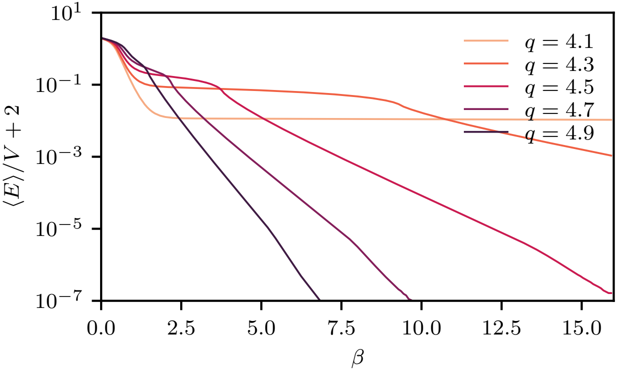

Figure: Energy density (logscale) from TRG with volume 1024×1024.

Choice of φ_0

- Choice of φ_0 can change the DOF in the model
- We choose $\varphi_0 = 0$, i.e. $\varphi \in [0, 2\pi)$, but we also investigate $\varphi_0 = -\pi$

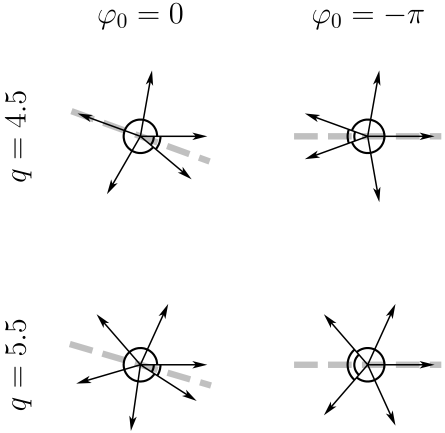

Phase diagram for $\gamma = \infty$ and $\varphi_0 = -\pi$

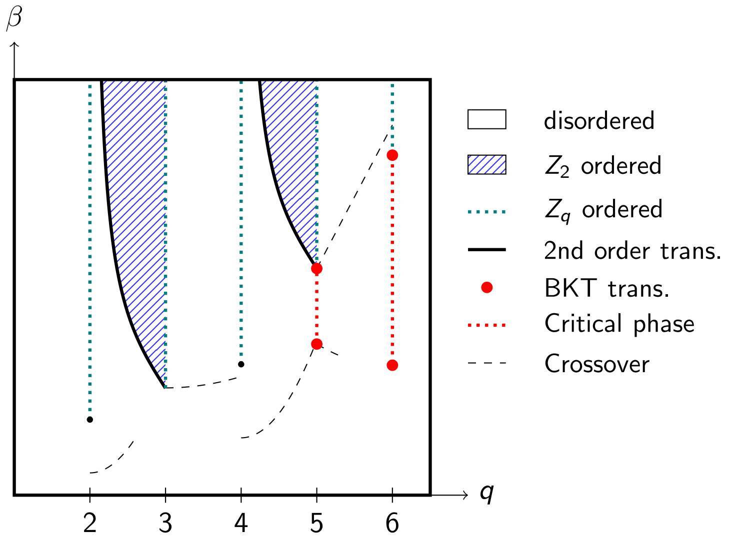

Effect of Angle Cutoff

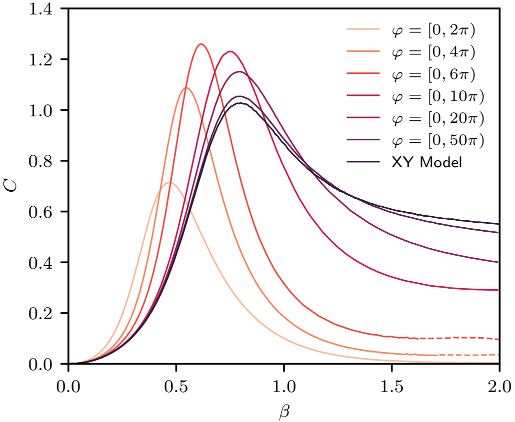

Figure: Specific heat for $q = 3.141592654$ with different cutoffs for the allowed angles. When the cutoff is removed (i.e. $\varphi \in (-\infty, \infty)$), all irrational q reduce to the XY model, and all rational $q = r/s$ reduce to the r-state ordinary clock model.

TRG Validation

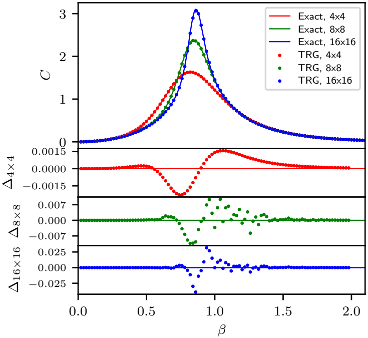

Figure: Comparison of specific heat calculated via exact and TRG for $q = 4.0$. Bottom panels show difference of TRG from exact.

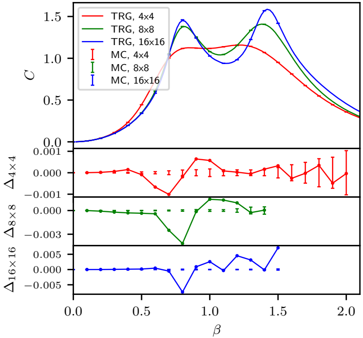

Figure: Comparison of specific heat calculated via MC and TRG for $q = 4.9$. Bottom panels show difference of TRG from MC with MC as baseline.

Autocorrelation

$$\tilde{\tau}_{X,int} = 1 + 2\sum_{t=1}^{T} \frac{C(t)}{C(0)} \quad \text{where} \quad C(t) = \langle X_i X_{i+t} \rangle - \langle X_i \rangle \langle X_{i+t} \rangle$$

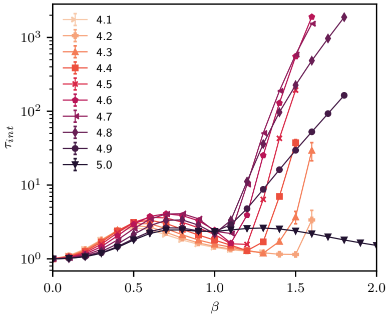

Figure: Integrated autocorrelation time for the energy density on a 4×4 lattice using heatbath algorithm.

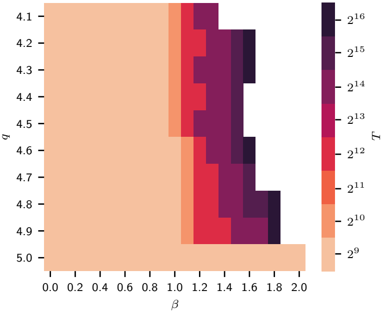

Figure: The values of T used to extract τ_{int}.

Some Monte Carlo results for $\gamma \to \infty$

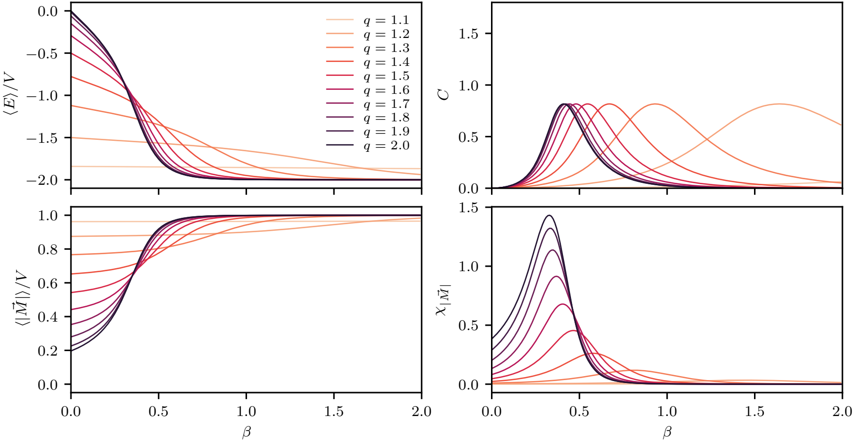

Figure: Results from a heatbath algorithm on a 4×4 lattice.

Some Monte Carlo results for $\gamma \to \infty$

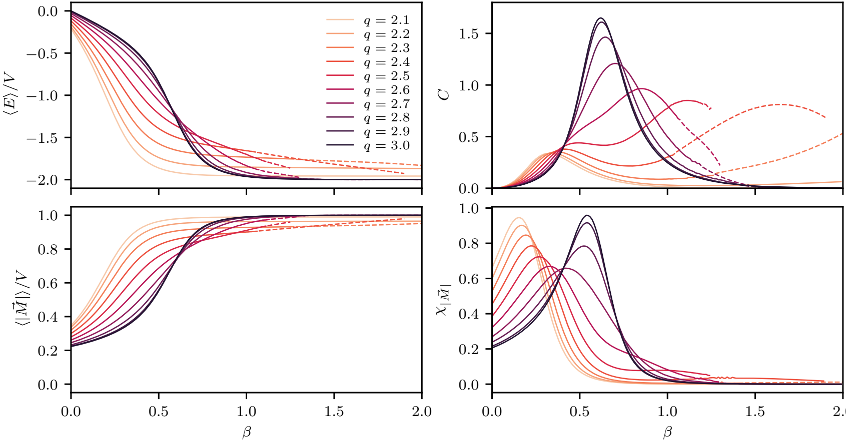

Figure: Results from a heatbath algorithm on a 4×4 lattice.

Some Monte Carlo results for $\gamma \to \infty$

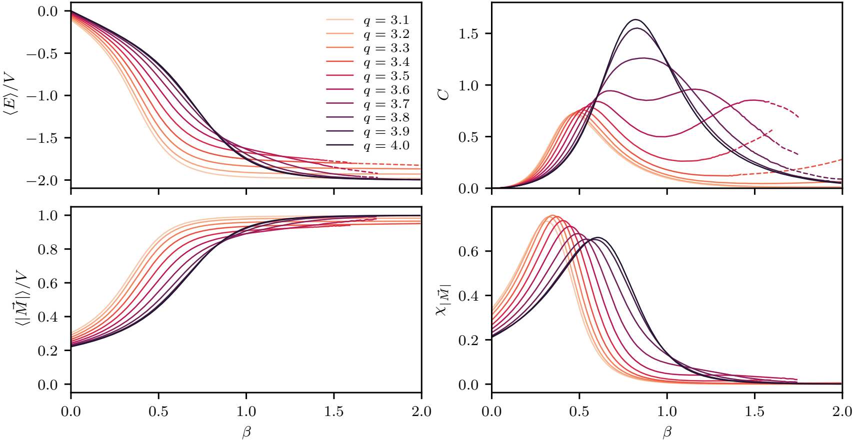

Figure: Results from a heatbath algorithm on a 4×4 lattice.

Some Monte Carlo results for $\gamma \to \infty$

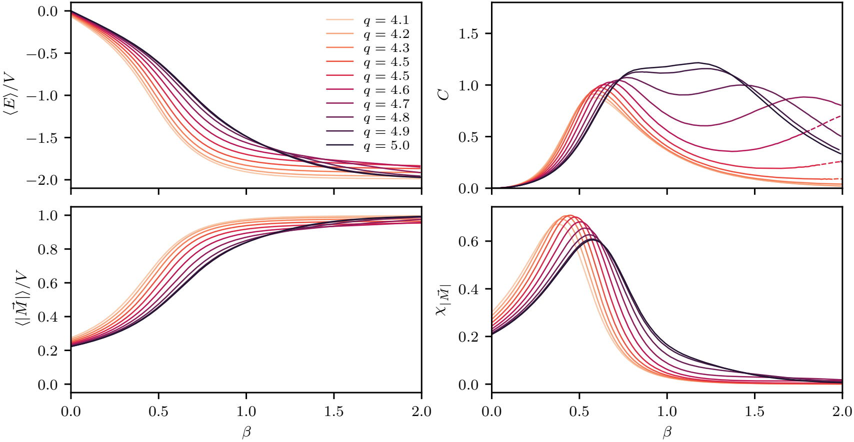

Figure: Results from a heatbath algorithm on a 4×4 lattice.

Some Monte Carlo results for $\gamma \to \infty$

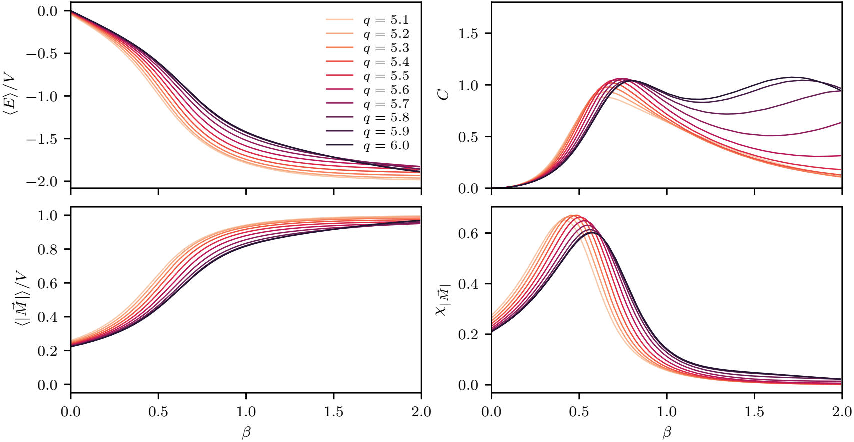

Figure: Results from a heatbath algorithm on a 4×4 lattice.